Journal of Materials Chemistry C

PAPER

View Article Online
View Journal | View Issue

Cite this: J. Mater. Chem. C, 2015, 3, 4663

The first blue phase reactive monomers containing a bi-mesogenic core and their side-chain polymers†

Chong-Lun Wei,[a] Yen-Ting Lin,[b] Jin-Huai Chang,[a] I-Hung Chiang[a] and Hong-Cheu Lin*[a]

Received 5th March 2015,
Accepted 30th March 2015

DOI: 10.1039/c5tc00615e

www.rsc.org/MaterialsC

Two novel blue phase (BP) reactive monomers **M1** and **M2** containing a bi-mesogenic core are first reported by introducing two end-attached acrylic spacers with different lengths. Due to the self-assembly of bi-mesogenic cores with the same side-by-side end-attached acrylate spacers in homopolymers **P1** and **P2**, no blue phase could be induced by homopolymerization of **M1** and **M2**. However, by interrupting the self-assembly of bi-mesogenic cores with different side-by-side spacer lengths of copolymers **P12**, double-twisted cylinders of BPIII could be further extended by copolymerization of **M1** and **M2** with different molar ratios. With **M1** : **M2** = 5 : 5 (molar ratio) in both side-chain copolymers **P12(soln:5/5)** and **P12(photo:5/5)** rather than binary mixture **M1/M2(5/5)**, the widest BPIII ranges of 5.3 °C and 3.8 °C could be obtained by solution- and photo-polymerization, respectively.

Introduction

In the last few decades, various liquid crystal molecules with many attractive mesophases have been obtained *via* special structural designs, including nematic,[1] smectic,[2] discotic,[3] and blue phases.[4–27] However, for liquid crystal scientists, blue phase liquid crystals (BPLCs) have aroused much attention as BPLCs have many exotic characteristics in the field of opto-electronics and photonics,[4] such as fast response time (about sub-milliseconds), no requirement of any alignment layer[5] and no birefringence.[6] Nowadays, BP molecular aggregates have been reported to possess internal helical alignment called the "double twisted cylinder (DTC)"[7] and they are classified as three types of BPs, *i.e.*, blue phases I, II, and III, where blue phase I (BPI) is a body-centered cubic structure, blue phase II (BPII) is a simple cubic structure and blue phase III (BPIII) has the same symmetry as the isotropic phase.[8] Although BPLCs have many benefits, they exhibited a very narrow temperature range (usually *ca.* 1 K), and were usually observed at high temperatures between the isotropic phase and the chiral nematic (N*) phase during the cooling process.[9] To overcome those disadvantages, many experts have tried some methods to stabilize BP structures and extend BP temperature ranges: Yang's group have shown that the liquid crystal oligomer could be self-assembled by hydrogen bonds, and it formed a BP complex with a wide temperature range about 23 °C.[10] Azobenzene dimers were also used to be doped into BPLCs to control the reflection wavelength.[11] Yoshizawa *et al.* used the structure of a binaphthyl unit to induce a blue phase and observed the BP temperature range approximately 30 °C.[12] In addition, a novel T-shaped chiral compound possessing a wide BP temperature range was also developed.[13] Photoisomerization was used to stabilize the liquid crystalline cubic blue phase by Takezoe *et al.*[14] and they connected a flexible linker between a rod and a cholesterol mesogenic unit which exhibited a wide range of BPs.[15] Oxadiazole-based bent-core liquid crystals were introduced to possess a blue phase with a wide mesophasic range *ca.* 30 °C.[16] Some researchers fabricated several biaxial nematic LCs doped with certain amounts of chiral dopants, which could enlarge the temperature range of BPs.[17] Besides, some groups used ZnS nanoparticles[18] or combined polymers and nanoparticles together to stabilize the BP.[19] Jiangang Lu *et al.* used polyaniline-functionalized graphene nanosheets to stabilize BPLCs and reduce their driving voltages.[20] Pivnenko *et al.* have reported that dimeric materials could stabilize the blue phase and enlarge its temperature range *ca.* 44 °C.[21] In the meanwhile, it is a very common idea and a helpful strategy to use polymeric structures to stabilize and extend the BP temperature ranges. For example, Kikuchi *et al.* have reported to stabilize and extend the temperature ranges of BPs over 60 °C by photo-polymerization of reactive monomers within the BP range of blue phase mixtures.[22] Dierking *et al.* used short-chain polystyrene to stabilize the BP

[a] Department of Materials Science and Engineering, National Chiao Tung University, Hsinchu, Taiwan. E-mail: linhc@mail.nctu.edu.tw
[b] Institute of Lighting and Energy Photonics, National Chiao Tung University, Tainan, Taiwan

† Electronic supplementary information (ESI) available. See DOI: 10.1039/c5tc00615e

temperature range up to 12 °C.[23] On the other hand, cyclosiloxane-based side chain co-polymers were reported by Zhang *et al.*, which had a wide BP temperature range.[24] Indeed, many experts extended the temperature ranges of BPs by simply using polymer networks to stabilize the BP dislocations.[25] As mentioned above, the BPs can be stabilized by doping and polymerization of reactive monomers in blue phase mixtures, which contain complicated components, including: nematic liquid crystals, chiral dopants, reactive monomers, and photo-initiators. Herein, we report the first type of BP reactive monomer successfully synthesized by introducing an acrylic end group into a previously reported BP LC diad. Through this way, the traditional polymerization technique of multiple components to stabilize the BP can be simplified to become a simple component system, *i.e.*, *via* polymerization of BP LC diads. Besides, in many studies only cubic BPs (BPI and BPII) can be locked by polymerization of reactive monomers in the desired mesophsic range due to the stabilization of dislocation lines in cubic BPs. Meanwhile, we first introduced BPIII reactive monomers and extended the temperature range of BPIII by solution- and photo-polymerization. Moreover, BPIII is believed to have an arbitrary orientation (isotropic symmetry) structure, so BPIII could be stabilized in the isotropic state. The diad structures of BPLCs have been reported by our group recently,[26] which are novel asymmetrical liquid crystal diads with a central chiral flexible linker to link two different mesogenic cores. As shown in Scheme 1, the first BP reactive monomers (diads **M1** and **M2** with different acrylate spacer lengths) are newly developed to possess an odd number asymmetrical chiral linker to form a biaxial bent-shaped structure to stabilize BPs. Presently, very few BP bent-shaped side-chain copolymers have been synthesized so far. Accordingly, both BPIII reactive monomers **M1** and **M2** are copolymerized *via* solution- and photo-polymerization to produce the first BP bent-shaped side-chain copolymers (**P12** with different molar ratios of **M1** and **M2**, see Scheme 1) in this study.

Experimental

Spectroscopic analysis

^{1}H NMR spectra were recorded on a Bruker Unity 300 MHz spectrometer using DMSO-d_6, $CDCl_3$ and THF-d_8 as solvents. Elemental analyses (EA) were performed on a Heraeus CHN-OS RAPID elemental analyzer. The molecular weights of polymers were obtained *via* gel permeation chromatography (GPC) measurements, which were carried out at 40 °C on a Waters 1515 instrument equipped with three Waters μ-Styragel columns (103, 104 and 105 Å) in series and a RI detector (ERMA Inc., ERC-7522). All GPC data were acquired by using tetrahydrofuran (THF) as the eluent at a flow rate of 1.0 mL min^{-1} and polystyrene samples as the molecular weight standards.

Liquid-crystalline and physical properties

The phase transition behaviors of all final asymmetrical diads were characterized by polarizing optical microscopy (POM) using a Leica DMLP equipped with a temperature control hot stage (Mettler Toledo FP82HT). Temperatures and enthalpies of phase transitions were determined by differential scanning calorimetry (DSC, model: Perkin Elmer Pyris 7) under N_2 at a heating and cooling rate of 1 °C min^{-1}.

Preparation of materials

All chemicals and solvents were of reagent grade and purchased from ACROS, Aldrich, TCI, Fluka, and TEDIA. THF was distilled over sodium/benzophenone to keep it anhydrous before use. After distillation over CaH_2, DMF was purified by refluxing with calcium hydride and then distilled. Azobisisobutyronitrile (AIBN) was recrystallized from methanol before use. The other chemicals were used without further purification. The monomers of **M1** and **M2** were synthesized following the already published procedure. The reactive monomers **M1** and **M2** of appropriate molar ratios were heated to the isotropic state at 80 °C, and then they were irradiated with a UV light of 1.5 mW cm^{-2}

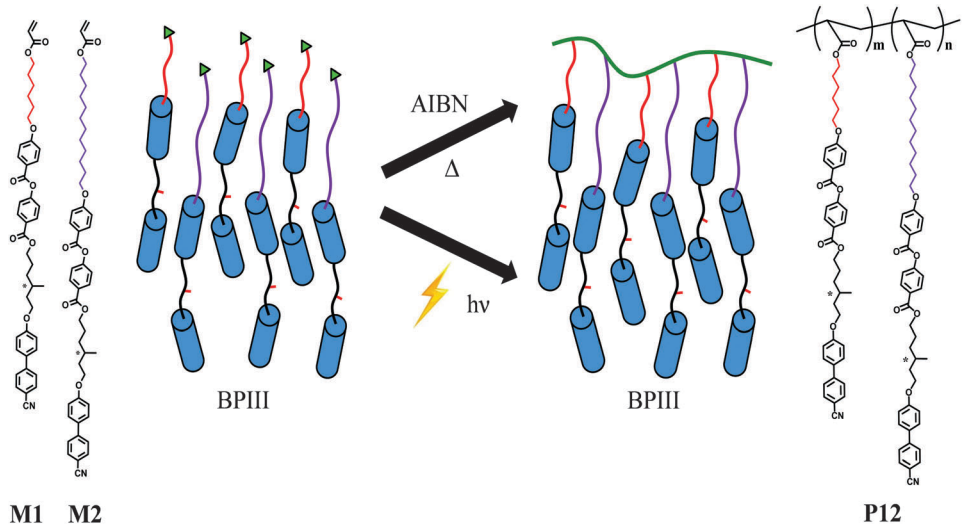

Scheme 1 Synthetic routes of blue phase (BP) side-chain copolymers **P12** by BP reactive monomers **M1** and **M2** with different acrylate spacer lengths.

at 365 nm with an exposure time of 20 min. The distance between the lamp and samples is 15 cm.

Synthesis of (*S*)-6-((4′-cyano-[1,1′-biphenyl]-4-yl)oxy)-4-methylhexyl 4-((4-((6-(acryloyloxy)hexyl)oxy)benzoyl)oxy)benzoate, M1. Yield: 78%. ^{1}H NMR (300 MHz, $CDCl_3$): δ (ppm) 8.02 (t, J = 8.5 Hz, 4H), 7.81 (s, 4H), 7.68 (d, J = 8.8 Hz, 2H), 7.36 (d, J = 8.7 Hz, 2H), 7.11 (d, J = 9.0 Hz, 2H), 7.04 (d, J = 8.8 Hz, 2H), 6.32 (m, 1H), 6.17 (m, 1H), 5.93 (m, 1H), 4.30 (t, J = 6.3 Hz, 2H), 4.11 (m, 6H), 1.75 (m, 6H), 1.66 (m, 4H), 1.43 (m, 7H), 0.97 (d, J = 6.3 Hz, 3H). Anal. calcd for $C_{43}H_{45}NO_8$: C, 72.69, H, 6.22, N, 1,82; found: C, 73.38, H, 6.44, N, 1.99%.

Synthesis of (*S*)-6-((4′-cyano-[1,1′-biphenyl]-4-yl)oxy)-4-methylhexyl 4-((4-((12-(acryloyloxy)dodecyl)oxy)benzoyl)oxy)benzoate, M2. Yield: 76%. ^{1}H NMR (300 MHz, $CDCl_3$): δ (ppm) 8.02 (t, J = 8.1 Hz, 4H), 7.81 (s, 4H), 7.68 (d, J = 8.6 Hz, 2H), 7.35 (d, J = 8.5 Hz, 2H), 7.10 (d, J = 9.0 Hz, 4H), 7.05 (d, J = 8.8 Hz, 2H), 6.31 (m, 1H), 6.16 (m, 1H), 5.92 (m, 1H), 4.29 (t, J = 6.3 Hz, 2H), 4.08 (m, 6H), 1.75 (m, 6H), 1.59 (m, 5H), 1.42 (m, 2H), 1.26 (m, 15H), 0.97 (d, J = 6.0 Hz, 3H). Anal. calcd for $C_{49}H_{57}NO_8$: C, 74.38, H, 7.39, N, 1,69; found: C, 74.69, H, 7.29, N, 1.78%.

All of the polymerization processes were carried out by free radical polymerization described as follows: to a Schlenk tube, monomers **M1** and **M2** were mixed at appropriate molar ratios (0 : 10, 9 : 1, 3 : 7, 5 : 5, 7 : 3, 1 : 9 and 10 : 0) dissolved in dry chlorobenzene (0.146 M) and AIBN (0.03 eq.) as an initiator. The solution was degassed by three freeze–pump–thaw cycles and then sealed off. The reaction mixture was stirred and heated at 60 °C for 24 h. After polymerization, the polymer was precipitated into diethyl ether for homo- and co-polymers. The precipitated polymers were collected, washed with diethyl ether, and dried under high vacuum.

P12(soln:5/5) (m/n = 5/5) ^{1}H NMR (300 MHz, $CDCl_3$): δ (ppm): 8.00 (br, 4H), 7.57–7.45 (m, 6H), 7.14 (br, 2H), 6.91 (m, 4H), 4.29–4.00 (m, 8H), 1.78–1.54 (br, 10H), 1.26–1.03 (br, 17H). M_n: 303, 541 g mol^{-1}, PDI: 1.27 M_w/M_n.

Results and discussion

Chemical synthesis

The synthetic procedures of both BPIII reactive monomers **M1** and **M2** are summarized in Scheme 2. The final chemical structures of monomers and polymers were confirmed by ^{1}H NMR spectra, and the weight average molecular weights (M_w) and polydispersity indexes (PDI) of polymers (see Table S1 of the ESI†) were determined by gel permeation chromatography (GPC).

NMR spectral studies

As shown in Fig. 1, the ^{1}H NMR spectra of copolymers show the disappearance of proton peaks in the region of vinyl acrylate groups with chemical shifts at 5.5–6.5 ppm (denoted as A, B, and C peaks), which indicated that all monomers were reacted completely by solution- or photo-polymerization and most sharp peaks became broader. The other related NMR data are also shown in Fig. S1 of the ESI.†

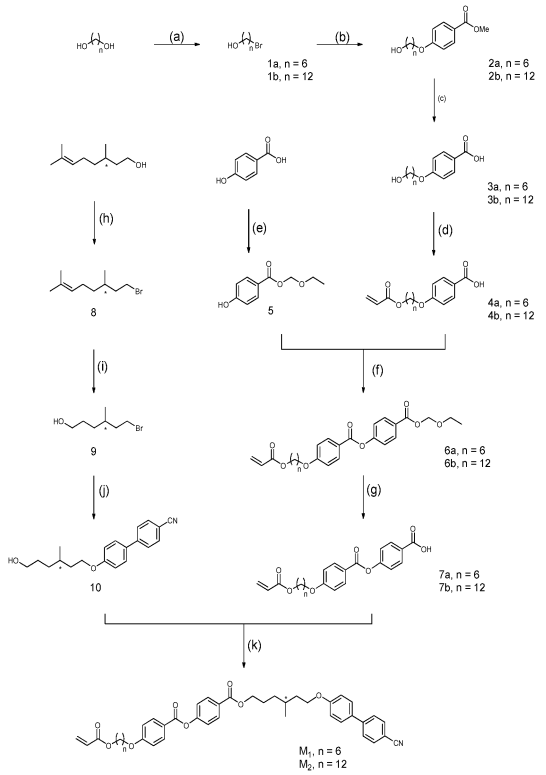

Scheme 2 Synthetic routes of blue phase reactive monomers **M1** and **M2**. *Reagents and conditions*: (a) HBr (48% in water), toluene, reflux, 18 h; (b) K_2CO_3, KI, acetone, reflux, 24 h; (c) KOH, MeOH, reflux, overnight; (d) acryloyl chloride, 1,4-dioxane, 45 °C, 3 h; (e) chloromethyl ethyl ether, 0 °C, DCM; (f) EDC, DMAP, DMF, r.t., 6 h; (g) PPTS, EtOH, 50 °C; (h) CBr_4, DCM, PPh_3, 0 °C, 4 h; (i) O_3, MeOH, 0 °C, 30 min, $NaBH_4$, MeOH, 2 h; (j) K_2CO_3, KI, acetone, reflux, 18 h; (k) EDC, DMAP, DCM, r.t., 24 h.

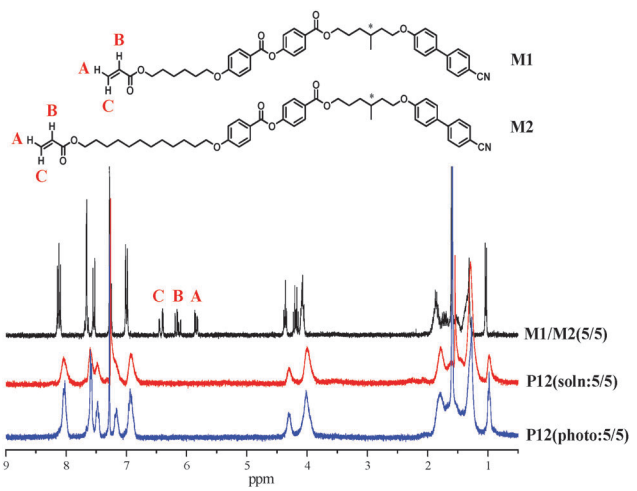

Fig. 1 ^{1}H NMR spectra of **M1**/**M2(5/5)**, **P12(soln:5/5)**, and **P12(photo:5/5)**.

Mesophasic and thermal properties

The mesophasic properties of these BP reactive monomers (**M1** and **M2**), copolymers (**P12** with various molar ratios of **M1** and **M2** viasolution- and photo-polymerization) and binary mixtures (**M1**/**M2** with various molar ratios of **M1** and **M2**) are

Table 1 Phase transition properties of solution-polymerization[a]

Compounds	Mole ratio (**M1**/**M2**)[b] Feeding	Output	Solution-polymerization Phase transition temperature[c,d] (°C) [enthalpies (J g^{-1})]	ΔT_{BP}
P1(soln)	10 : 0	10 : 0	Iso 143.7 [0.79] N* 131[e] G	0
P12(soln:9/1)	9 : 1	8.4 : 1.6	Iso 141.6 [0.77] BPIII 140.1[e] N* 126[e] G	1.5
P12(soln:7/3)	7 : 3	7 : 3	Iso 139.5 [0.85] BPIII 135.2[e] N* 114[e] G	4.3
P12(soln:5/5)	5 : 5	5 : 5	Iso 149.2 [0.71] BPIII 143.9[e] N* 131[e] G	5.3
P12(soln:3/7)	3 : 7	3 : 7	Iso 152.5 [1.02] BPIII 149.5[e] N* 124[e] G	3.0
P12(soln:1/9)	1 : 9	1.3 : 8.7	Iso 152.0 [0.94] BPIII 150.8[e] N* 139[e] G	1.2
P2(soln)	0 : 10	0 : 10	Iso 157.5 [1.03] N* 142[e] G	0

[a] Polymerized at 60.0 °C using AIBN. [b] **M1**: Iso 73.3 [0.82] BPIII 70.3 N* 41.6 [1.63] Cr; **M2**: Iso 73.5 [0.88] BPIII 71.1 N* 32.4 [1.70] Cr. [c] Peak temperatures in the DSC profiles obtained during the first heating and cooling cycles at a rate of 1 °C min^{-1}. [d] Iso = isotropic state; BPIII = blue phase III; N* = chiral nematic phase; G = glassy state. [e] The transition temperature was observed by POM due to undetectable DSC data.

Table 2 Phase transition properties of photo-polymerization[a]

Compounds	Photo-polymerization Phase transition temperature[b,c] (°C) [enthalpies (J g^{-1})]	ΔT_{BP}
Pl(photo)	Iso 143.0 [0.70] N* 132[d] G	0
P12(photo:9/1)	Iso 140.8 [0.92] BPIII 139.4[d] N* 129[d] G	1.4
P12(photo:7/3)	Iso 134.9 [0.80] BPIII 132.0[d] N* 110[d] G	2.9
P12(photo:5/5)	Iso 135.5 [0.75] BPIII 131.7[d] N* 121[d] G	3.8
P12(photo:3/7)	Iso 138.0 [0.85] BPIII 135.9[d] N* 111[d] G	2.1
P12(photo:1/9)	Iso 139.2 [0.95] BPIII 138.4[d] N* 131 [d] G	0.8
P2(photo)	Iso 153.7 [0.98] N* 142[d] G	0

[a] Polymerized at 80 °C in the isotropic state. [b] Peak temperatures in the DSC profiles obtained during the first heating and cooling cycles at a rate of 1 °C min^{-1}. [c] Iso = isotropic state; BPIII = blue phase III; N* = chiral nematic phase; G = glassy state. [d] The transition temperature was observed by POM due to undetectable DSC data.

summarized in Tables 1–3. The phase transition of the isotropic phase (Iso)-foggy blue color phase (BPIII)-chiral nematic phase (N*)-glassy state (G) was determined by polarizing optical microscopy (POM) and enthalpy changes were determined by differential scanning calorimetry (DSC). The BP reactive monomer **M1** containing a six carbon number end-attached acrylate spacer possesses a mesophasic BPIII range of 3.0 °C. However, as shown in Table 1 the BPIII phase of **M1** was eliminated by solution-polymerization of **M1** to generate homopolymer **P1(soln)**, where the mesophasic behaviour of **P1(soln)** only demonstrated the isotropic phase (Iso) – chiral nematic phase (N*) – glassy state (G).

Table 3 Phase transition properties of binary mixtures[a,b]

Compounds	Phase transition temperature (°C) [enthalpies (J g^{-1})]	ΔT_{BP}
Ml	Iso 73.3 [0.82] BPIII 70.3[c] N* 41.6 Cr	3.0
M1/M2(9/1)	Iso 74.3 [0.83] BPIII 71.7[c] N* 38.1 Cr	2.6
M1/M2(7/3)	Iso 74.5 [0.96] BPIII 72.1[c] N* 35.2 Cr	2.4
M1/M2(5/5)	Iso 74.7 [0.75] BPIII 72.7[c] N* 38.4 Cr	2.0
M1/M2(3/7)	Iso 73.6 [0.86] BPIII 71.1[c] N* 35.8 Cr	2.5
M1/M2(1/9)	Iso 73.7 [0.95] BPIII 71.0[c] N* 34.4 Cr	2.7
M2	Iso 73.5 [0.88] BPIII 71.1[c] N* 32.4 Cr	2.4

[a] Peak temperatures in the DSC profiles obtained upon the first cooling and second heating cycles at a rate of 1 °C min^{-1}. [b] Iso = isotropic state; BPIII = blue phase III; N* = chiral nematic phase; Cr = crystal. [c] The transition temperature was observed by POM due to undetectable DSC data.

Similar to the previous monomer design, **M2** possessing a longer end-attached acrylate spacer with a carbon number of twelve revealed a mesophasic range of 2.4 °C for BPIII. Unfortunately, the homopolymer **P2(soln)** solution polymerized by **M2** cannot exhibit BPIII either (see Table 1). The disappearance of BPIII in homopolymers **P1(soln)** and **P2(soln)** might be attributed to the strong side-by-side self-assembly of the bi-mesogenic cores with the same lengths of end-attached acrylate spacers in the side-chain homopolymers.

In order to reduce the side-by-side self-assembly of the bi-mesogenic cores in the side-chain homopolymers, copolymerization of **M1** and **M2** with different acrylate spacer lengths might be a good strategy to reduce the side-by-side self-assembly of the bi-mesogenic cores. Hence, copolymers **P12** with various molar ratios of **M1** and **M2** were synthesized *via* solution-polymerization, which was initiated by azobis-isobutyronitrile (AIBN) at 60 °C, to reduce and their phase transition properties are illustrated in Table 1. Surprisingly, the side-chain copolymer **P12(soln:5/5)** with a 5 : 5 molar ratio of **M1** and **M2** displayed a widest mesophasic range of BPIII (5.3 °C) among all copolymers **P12**. This interesting result explained that the different lengths of end-attached acrylate spacers of **M1** and **M2** in copolymer **P12(soln:5/5)** might disturb the side-by-side self-assembly of the bi-mesogenic cores so that the bi-mesogenic cores on the side chains of copolymers can form double-twisted cylinders more easily. In addition, the other side-chain copolymers **P12(soln)** possess narrower mesophasic ranges of BPIII, where the narrowest mesophasic range of BPIII (1.2 °C) was observed in **P12(soln:1/9)**. Comparably, as shown in Table 2, photo-polymerization was carried out to acquire homopolymers **P1(photo)** and **P2(photo)** along with copolymers **P12(photo)** with various molar ratios of **M1** and **M2** at isotropic temperature (80 °C), where the radiation intensity was 1.5 mW cm^{-2} at 365 nm with an exposure time of 20 min. Similar to solution-polymerization, no BPIII was observed in **P1(photo)** and **P2(photo)**, and the widest and narrowest mesophasic ranges of BPIII (3.8 and 1.2 °C) were observed in **P12(photo:5/5)** and **P12(photo:1/9)**, respectively. In general, all side-chain copolymers **P12** possess broader mesophasic ranges of BPIII *via* solution-polymerization than photo-polymerization, which might be due to the higher molecular weights obtained *via* solution-polymerization than photo-polymerization (see Table S1 and Fig. S2 in ESI†).

In the meantime, the binary mixtures of **M1** and **M2** (*i.e.*, **M1/M2**) with different molar ratios were prepared to compare with their side-chain copolymers **P12(soln)** and **P12(photo)** possessing analogous compositions, and the phase transition properties of binary mixtures **M1/M2** are illustrated in Table 3.

Though all binary mixtures **M1/M2** possessed BPIII, narrower BPIII ranges were observed in these binary mixtures in contrast to **M1**. Thus, the BPIII ranges of **M1** and **M2** could not be further extended by the strategy of using binary mixtures, which is totally different from the copolymerization strategy to enhance BPIII ranges, *e.g.*, homopolymers **P1** and **P2** without BPIII *vs.* copolymers **P12** with BPIII. Particularly, the BPIII range (5.3 °C) of copolymer **P12(soln:5/5)** is wider than that (2.0 °C) of binary mixture **M1/M2(5/5)** with a molar ratio of 5 : 5. This result might be explained by the fact that the side-by-side self-assembly of the bi-mesogenic cores could be disrupted by copolymerization of two monomers with different acrylate spacer lengths, which did not occur to the binary mixture of monomers **M1** and **M2** without the linkage of polymer backbones. All related DSC curves and BP ranges of binary mixtures, photo- and solution-polymerization processes are illustrated in Fig. S3 and S4 (ESI†), respectively, of the ESI.†

Optical investigation

The **M1/M2(5/5)** behavior of BPIII could be verified by the rotation of a polarizer (see Fig. 2). As the polarizer was rotated clockwise by a small angle of 10° from the crossed position, the color was changed from blue to light blue (Fig. 2(a)). Upon rotating the polarizer counterclockwise by the same angle (10°) from the crossed position, the color was changed from blue to red (Fig. 2(c)). The POM observations also indicated that the phase of BPIII has selective reflection colors according to their pitch lengths, which were examined by changing the cross angles in the polarizer and analyzer of POM. As shown in Fig. 3(a)–(c), the similar consequence could be observed in **P12(soln:5/5)**.

AFM morphology studies

In order to analyze the morphological surface structure of the blue phase clearly, **P12(soln:5/5)** with the broadest BPIII mesophasic range was quenched from different states, including: the isotropic state, and BPIII and N* phases, through rapid immersion into liquid N_2 to supercool and maintain their frozen textures.

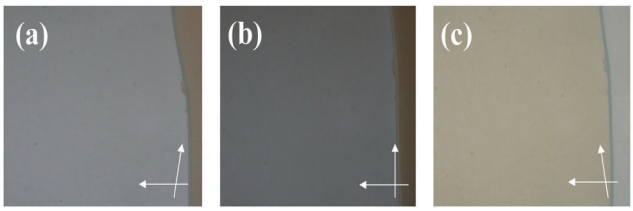

Fig. 2 The chirality behaviors of **M1/M2(5/5)** observed by POM at 73.5 °C. (a) The polarizer was rotated clockwise by a small angle of 10°; (b) the polarizer and analyzer were orthogonal; (c) the polarizer was rotated counterclockwise by a small angle of 10°. (White arrows are the directions of polarizers and analyzers.)

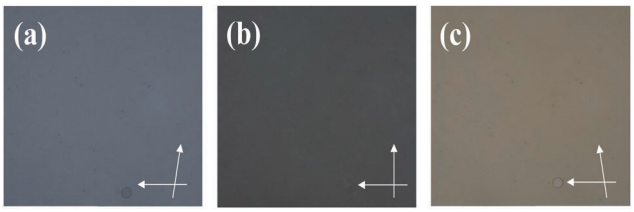

Fig. 3 The chirality behaviors of **P12(soln:5/5)** observed by POM at 146.1 °C. (a) The polarizer was rotated clockwise by a small angle of 10°; (b) The polarizer and analyzer were orthogonal; (c) the polarizer was rotated counterclockwise by a small angle of 10°. (White arrows are the directions of polarizers and analyzers.)

The photo images of POM and atomic force microscopy (AFM) are displayed in Fig. 4(a)–(f), respectively. In contrast to an unclear and random texture of Fig. 4(d) in the isotropic state, the irregular filamentous structure of BPIII is shown in Fig. 4(e), in which the filamentary texture is arranged in random orientations with diameters *ca.* 2–5 nm and lengths *ca.* 0.1–0.5 μm. An expanded AFM image of **P12(soln:5/5)** in

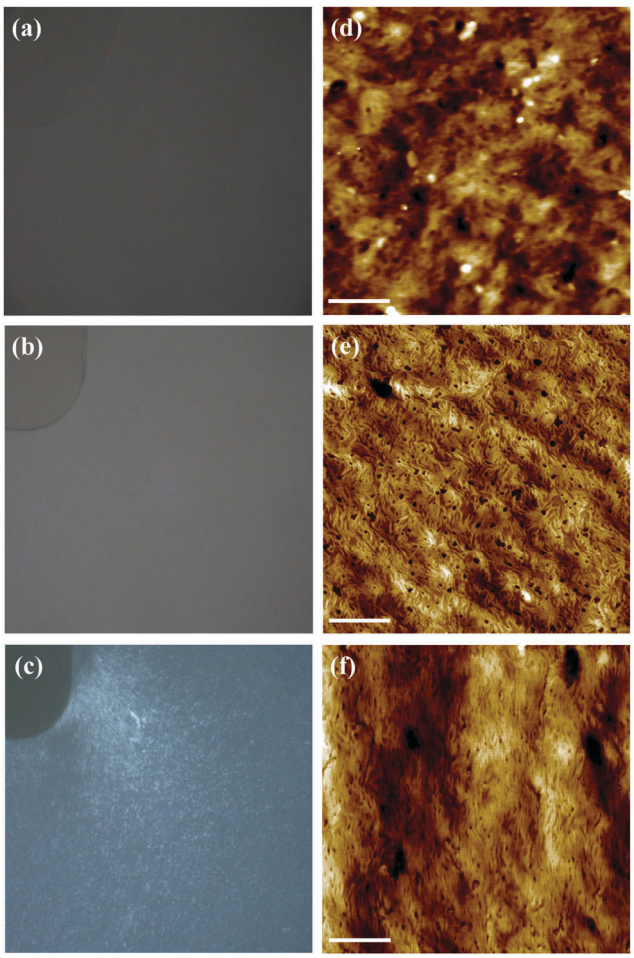

Fig. 4 POM textures of **P12(soln:5/5)** upon cooling (0.5 °C min^{-1}). (a) Isotropic state at 155 °C. (b) Blue phase III at 146.1 °C. (c) Chiral nematic phase at 138.7 °C. AFM images of **P12(soln:5/5)** was quenched by liquid N_2; (d) isotropic state at 155 °C. (e) Blue phase III at 146.1 °C. (f) Chiral nematic phase at 138.7 °C. (White scale bar: 1 μm.)

BPIII is demonstrated in Fig. S5 of the ESI.† Compared with the highly ordered structures of BPI (body-center cubic structure) and BPII (simple cubic structure), the structure of BPIII is predicted to be more symmetric as the isotropic state and to become amorphous with the short-range order of double twisted structure alone. As shown in the AFM image of Fig. 4(e) and Fig. S5 (ESI†), the surface of BPIII exhibited an irregular array and the cylindrical shaped objects were arranged in oblique and fractured filaments with random orientations. They have also been found to exhibit similar morphological images of spaghetti-like tangles and liquid-like arrangements in BPIII.[27] Upon further cooling, Fig. 4(f) with the disappearance of BPIII only demonstrates a liquid-like surface in N* due to lack of the double twisted cylindrical structure.

Conclusions

In summary, we have developed the first BP reactive monomers possessing the bi-mesogenic core containing one central chiral linker. By introducing two end-attached acrylic spacers with different lengths (*i.e.*, carbon number = 6 and 12 for **M1** and **M2**, respectively) into the first BP reactive monomers, the blue phase (BPIII) ranges of copolymers could be further extended and stabilized by solution- and photo-polymerization of **M1** and **M2**, with a molar ratio of 5 : 5. Instead of photo-polymerization of double-twisted cylinders to stabilize the BP structure, this approach is also the first ever tried solution-polymerization (instead of photo-polymerization only) of monomers to produce the BP LCs. However, due to the strong side-by-side self-assembly of the bi-mesogenic cores with the same lengths of end-attached acrylate spacers in the side-chain homopolymers **P1** and **P2**, the homopolymerization of **M1** and **M2** could not induce any blue phase. Besides, the morphological surface structure of the irregular filamentous- and spaghetti-like tangled BPIII was first observed in copolymer **P12(soln:5/5)** by AFM in this report. This research opens up a new avenue for designing novel reactive monomers and polymers that can stabilize the blue phase efficiently. Accordingly, this report also offers blue phase reactive monomers for the first time as suitable dopant candidates of multi-component LC mixtures to stabilize BPs for the future display applications.

Acknowledgements

The financial support of this project is provided by the Ministry of Science and Technology (MOST) in Taiwan through MOST 103-2113-M-009-018-MY3 and MOST 103-2221-E-009-215-MY3.

Notes and references

1 (*a*) D. Y. Kim, S. A. Lee, H. J. Choi, L. C. Chien, M. H. Lee and K. U. Jeong, *J. Mater. Chem. C*, 2013, **1**, 1375; (*b*) W. Nishiya, Y. Takanishi, J. Yamamotob and A. Yoshizawa, *J. Mater. Chem. C*, 2014, **2**, 3677.
2 W. H. Chen, W. T. Chuang, U. S. Jeng, H. S. Sheu and H. C. Lin, *J. Am. Chem. Soc.*, 2011, **133**, 15674.
3 D. Y. Kim, S. A. Lee, Y. J. Choi, S. H. Wang, S. W. Kuo, C. Nah, M. H. Lee and K. U. Jeong, *Chem. – Eur. J.*, 2014, **20**, 5689.
4 (*a*) Y. H. Lin, H. S. Chen, H. C. Lin, Y. S. Tsou, H. K. Hsu and W. Y. Li, *Appl. Phys. Lett.*, 2010, **96**, 113505; (*b*) Y. H. Lin, H. S. Chen, T. H. Chiang, C. H. Wu and H. K. Hsu, *Opt. Express*, 2011, **19**, 2556.
5 C. L. Rao, Z. Ge, S. Gauza, K. M. Chen and S. T. Wu, *Mol. Cryst. Liq. Cryst.*, 2010, **527**, 30.
6 Z. Ge, S. Gauza, M. Jiao, H. Xianyu and S. T. Wu, *Appl. Phys. Lett.*, 2009, **94**, 101104.
7 (*a*) H. S. Kitzerow and P. P. Crooker, *Phys. Rev. Lett.*, 1991, **67**, 2151; (*b*) R. M. Hornreich, *Phys. Rev. Lett.*, 1991, **67**, 2155; (*c*) H. Kikuchi, *Struct. Bonding*, 2008, **128**, 99.
8 (*a*) O. Henrich, K. Stratford, M. E. Cates and D. Marenduzzo, *Phys. Rev. Lett.*, 2011, **106**, 107801; (*b*) A. Yoshizawa, *RSC Adv.*, 2013, **3**, 25475.
9 (*a*) H. S. Kitzerow, *ChemPhysChem*, 2006, **7**, 63; (*b*) P. P. Crooker, in *Chirality in Liquid Crystals*, ed. H. S. Kitzerow and C. Bahr, Springer, New York, 2001, ch. 7, p. 186.
10 W. He, G. Pan, Z. Yang, D. Zhao, G. Niu, W. Huang, X. Yuan, J. Guo, H. Cao and H. Yang, *Adv. Mater.*, 2009, **21**, 2050.
11 X. Chen, L. Wang, C. Li, J. Xiao, H. Ding, X. Liu, X. Zhang, W. He and H. Yang, *Chem. Commun.*, 2013, **49**, 10097.
12 A. Yoshizawa, Y. Kogawa, K. Kobayashi, Y. Takanishi and J. Yamamoto, *J. Mater. Chem.*, 2009, **19**, 5759.
13 A. Yoshizawa, M. Sato and J. Rokunohe, *J. Mater. Chem.*, 2005, **15**, 3285.
14 M. J. Gim, S. T. Hur, K. W. Park, M. Lee, S. W. Choi and H. Takezoe, *Chem. Commun.*, 2012, **48**, 9968.
15 S. Aya, A. Zep, K. Aihara, K. Ema, K. Pociecha, E. Gorecka, F. Araoka, K. Ishikawa and H. Takezoe, *Opt. Mater. Express*, 2014, **4**, 662.
16 I. H. Chiang, C. J. Long, H. C. Lin, W. T. Chuang, J. J. Lee and H. C. Lin, *ACS Appl. Mater. Interfaces*, 2014, **6**, 228.
17 (*a*) S. Taushanoff, K. Van Le, J. Williams, R. J. Twieg, B. K. Sadashiva, H. Takezoe and A. Jákli, *J. Mater. Chem.*, 2010, **20**, 5893; (*b*) M. Lee, S. T. Hur, H. Higuchi, K. Song, S. W. Choi and H. Kikuchi, *J. Mater. Chem.*, 2010, **20**, 5813; (*c*) I. Dierking, W. Blenkhorn, E. Credland, W. Drake, R. Kociuruba, B. Kayser and T. Michael, *Soft Matter*, 2012, **8**, 4355.
18 L. Wang, W. He, X. Xiao, F. Meng, Y. Zhang, P. Yang, L. Wang, J. Xiao, H. Yang and Y. Lu, *Small*, 2012, **8**, 2189.
19 L. Wang, W. He, Q. Wang, M. Yu, X. Xiao, Y. Zhang, M. Ellahi, D. Zhao, H. Yang and L. Guo, *J. Mater. Chem. C*, 2013, **1**, 6526.
20 S. Ni, H. Li, S. Li, J. Zhu, J. Tan, X. Sun, C. P. Chen, G. D. Wu, K. C. Lee, C. C. Lo, A. Lien, J. Lu and Y. Su, *J. Mater. Chem. C*, 2014, **2**, 1730.
21 H. J. Coles and M. N. Pivnenko, *Nature*, 2005, **436**, 997.
22 H. Kikuchi, M. Yokota, Y. Hisakado, H. Yang and T. Kajiyama, *Nat. Mater.*, 2002, **1**, 64.

23 N. Kasch, I. Dierking and M. Turner, *Soft Matter*, 2013, **9**, 4789.
24 B. Y. Zhang, F. B. Meng and Y. H. Cong, *Opt. Express*, 2007, **15**, 10175.
25 (*a*) E. Kemiklioglu, J. Y. Hwang and L. C. Chien, *Phys. Rev. E: Stat., Nonlinear, Soft Matter Phys.*, 2014, **89**, 042502; (*b*) Y. Chen, D. Xu, S. T. Wu, S. Yamamoto and Y. Haseba, *Appl. Phys. Lett.*, 2013, **102**, 141116; (*c*) Y. F. Lan, C. Y. Tsai, L. Y. Wang, P. J. Ku, T. H. Huang, C. Y. Liu and N. Sugiura, *Appl. Phys. Lett.*, 2012, **100**, 171902.
26 C. L. Wei, T. C. Chen, P. Raghunath, M. C. Lin and H. C. Lin, *RSC Adv.*, 2015, **5**, 4615.
27 J. A. N. Zasadzinski, S. Meiboom, M. J. Sammon and D. W. Berreman, *Phys. Rev. Lett.*, 1986, **57**, 364.